PREDICTION OF CRACKS CAUSED BY AUTOGENOUS SHRINKAGE AND DRYING SHRINKAGE

(Translation from Proceedings of JSCE, No.662/V-49, November 2000)

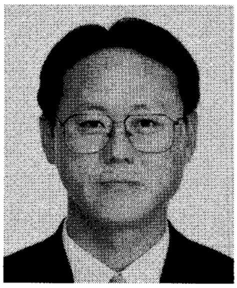

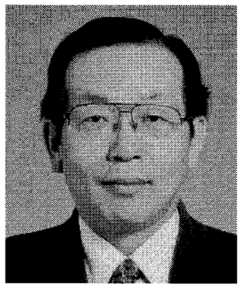

Toshio OHNO　　Taketo UOMOTO

As a part of an investigation related to predicting the time at which cracking occurs, cracks are induced in concrete specimens by imposing uni-axial restraint and subjecting them to conditions that cause volume changes. The influence of various factors on the time of cracking, the behavior of strain around crack locations, and the potential for using the tensile strain capacity and the ratio of shrinkage stress to tensile strength as the critical cracking index are investigated. A comparison of an analytical approach with the experimental results is also investigated. As a result that, it is shown that non-uniform shrinkage strain in the cross section is the cause of variation in time of cracking. It is also demonstrated that the tensile strain capacity calculated in influencing area on cracking and the ratio of shrinkage stress to tensile strength are applicable in a practical sense as critical limit criteria for the prediction of cracking time.

Keywords: drying shrinkage, autogenous shrinkage, time of cracking, critical cracking limit, tensile strain capacity, ratio of shrinkage stress to tensile strength

---

Toshio Ohno is a chief research engineer in the Department of Civil Engineering at Kajima Technical Research Institute, Tokyo, Japan. His research interests relate to cracking phenomena and the durability of concrete and asphalt mixtures. He is a member of the JSCE.

Taketo Uomoto is a Director and Professor of the International Center for Urban Safety Engineering and the Institute of Industrial Science at the University of Tokyo, Japan. He obtained his D.Eng. from the University of Tokyo in 1981. His research interests relate to the durability of concrete, nondestructive testing, and new composite materials, as well as the rational mix design of shotcrete. He is a fellow of the JSCE.

1. INTRODUCTION

Cracks not only spoil esthetics of concrete structures, but also lead to water seepage. They form paths for the entry of corrosion-inducing chemicals and the oozing out of hydration products. The end result of the presence of these paths through the concrete may be a threat to the durability and performance of the structure.

Many cracks begin when shrinkage and/or expansion of the concrete is in some way restrained. Such volumetric changes may be caused by drying shrinkage, thermal stress, or rapid changes in temperature and/or humidity in the environment. Further, autogenous shrinkage of modern high-strength concretes and highly flowable concretes containing a large amount of powder may be a further cause of cracking. However, in actual concrete structures, there is seldom a single reason for cracks appearing; rather, they result from complex interactions between these various factors. This complexity leads to difficulty in estimating the strains and stresses acting on concrete. Further, in addition to these factors that cause volume changes to the concrete, the physical properties of concrete change with age while temperature, humidity, wind, and other environmental influences change by the minute. Consequently, as of the present time, it is impossible to predict precisely when cracking will occur in actual concrete structure [1].

On the other hand, there have been reports that a limit tensile stress that exceeds 80% of tensile strength in the case of thermal stress [2] or a shrinkage stress that exceeds from 60% to 70% of tensile strength in the case of drying shrinkage [3] [4] [5] can be considered a critical cracking limit.

The authors are investigating the influence of various volume-changing factors on the time at which cracking occurs. They are also studying the possibility of using the tensile strain capacity or the ratio of shrinkage stress to tensile strength as a measure for the critical cracking limit. This work is based on experiments in which specimens are imposed with a uni-axial restraint according to the standard modified JIS original [6] [7]. In this paper, further progress with these studies is described, in which analytical values calculated stepwise are compared against experimental values of shrinkage stress, leading to an evaluation of a prediction method for the time of cracking due to concrete volume changes.

2. EXPERIMENTAL PROGRAM

2.1 Experimental factors

Drying shrinkage cracks may result from a combination of such factors as material properties (type of cement, admixture and coarse aggregate), the concrete mix (unit water content, quantity of cement paste, and water-cement ratio), ambient condition (such as temperature and humidity), design/construction factors (such as shape and dimensions of members, types and degrees of restraints, and age at which drying begins). In this investigation, the most representative of these factors are adopted as independent parameters and these are regarded as having a significant influence on cracking due to volume changes: water-cement ratio, amount of coarse aggregate (amount of mortar), age at which drying begins, and degree of restraint (sectional area of restraint frame). The experimental parameters are detailed in Table 1.

Table 1 Combinations of experimental parameters

<table>
<tr><th>Experiment No.</th><th>Water-cement ratio (%)</th><th>Age when drying starts (day)</th><th>Sectional area of restraint frame (mm^2)</th><th>Amount of coarse aggregate (kg/m^3)</th></tr>
<tr><td>1</td><td>30</td><td rowspan="2">7</td><td rowspan="3">697</td><td rowspan="7">1,030</td></tr>
<tr><td>2</td><td>45</td></tr>
<tr><td>3</td><td rowspan="9">60</td><td>1</td></tr>
<tr><td>4</td><td rowspan="3">7</td><td>1,019</td></tr>
<tr><td>5</td><td>697</td></tr>
<tr><td>6</td><td>496</td></tr>
<tr><td>7</td><td>28</td><td>697</td></tr>
<tr><td>8</td><td rowspan="4">7</td><td>496</td><td>515</td></tr>
<tr><td>9</td><td>1,019</td><td rowspan="3">0</td></tr>
<tr><td>10</td><td>697</td></tr>
<tr><td>11</td><td>496</td></tr>
</table>

2.2 Test specimens and measurements

a) Restrained shrinkage cracking test

Various methods have been proposed for inducing shrinkage cracks in concrete specimens [8]. Here, uni-axial restraint with light-weight-ditch steel (light-weight-channel) is used according to the standard modified Japanese

Industrial Standard entitled "Testing method on cracking of concrete due to restrained drying shrinkage (draft)" [8] [9] for restrained shrinkage cracking tests. The shape and size of the restrained specimen is shown in Fig.1. The minimum cross section of the specimen is a 100 mm square, and there is a straight section 300 mm long with this cross section. A view of the shrinkage cracking test in progress is shown in Photo 1.

Brass studs for gauges were pasted onto the specimens immediately after demolding at regular intervals of 100 mm over a distance of 500 mm span on both the placing surface and the bottom as shown in Fig.1. Concrete strain was measured at intervals of one or two days by using a contact-type strain gauge (precision: 0.001mm) after drying. This was continued until such time as a penetrating crack was observed in each specimen. Here, the measuring points are labeled F-1 to F-5 from top down on the placing surface and B-1 to B-5 from the top down on the bottom, respectively. Five restraint specimens were cast for each case and examined for shrinkage cracking to derive reliable data.

Strain of restraint frame was automatically measured every three hours by wire strain gauges (gauge length: 3mm; four gauges per specimen) pasted on at the center of gravity of the cross section in middle height of right and left light-weight-channel. Again, measurements continued from initial setting until a penetrating crack was observed. The age at which cracking occurred was defined as the point when the strain in the restraint frame returned to almost zero.

Three free-shrinkage specimens of the same size but without the restraint frame were also prepared, and concrete strain was measured in the same way.

Three prism specimens measuring $100 \times 100 \times 400$ mm were also prepared to the test the autogenous shrinkage of concrete. The concrete strain during wet curing (before drying) was evaluated according to a report entitled "Testing method for autogenous shrinkage and autogenous expansion of cement paste, mortar, and concrete (draft)" by Japan Concrete Institute committee [10]. To do this, the length change of the concrete was measured from initial setting until the age at which drying began. The aluminum tape used to wrap the specimens was then stripped off, specimens were exposed to drying conditions, and testing began.

b) Test for physical properties
The fresh mix properties measured in the experiment were slump, air content, and hardening speed of mortar (JIS A 6204).

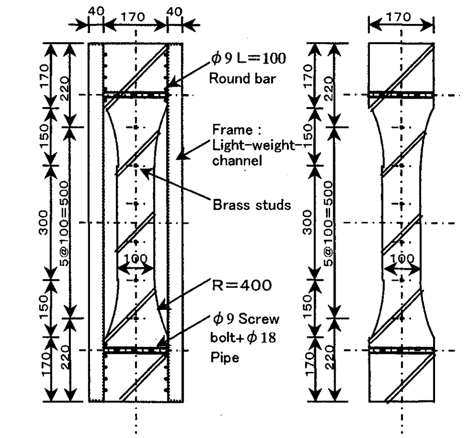

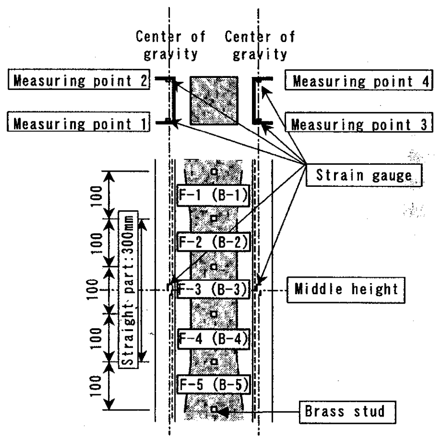

Strain measuring points

(F :Placing surface, B :Bottom side)

Fig.1 Shape and size of specimen (Unit: mm)

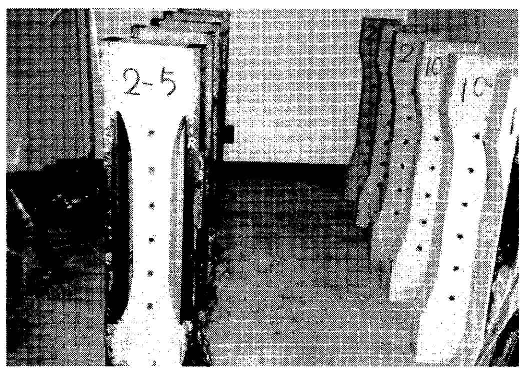

Photo 1 View of shrinkage cracking test

Compressive strength (JIS A 1108; $\phi 100 \times h200$), Young's modulus (JSCE G502; $\phi 100 \times h200$) and splitting tensile strength (JIS A 1113; $\phi 150 \times h200$) were measured at four ages: the age at which drying started, 28 days (except splitting tensile strength), and the age at which cracks were observed on first specimen in the five restrained specimens and last specimen in those specimens. All specimens were cured under wet conditions until drying began, and were then exposed to the same drying conditions as restrained specimens (except those cured in water).

2.3 Mix proportions

Various concrete and mortar mix proportions are listed in Table 2. Mixes for concrete with water-cement ratios of 30%, 45%, and 60% (C30, C45, C60) were designed such that they had the same water content (167kg/m^3) and amount of coarse aggregate (1,030kg/m^3). The mix proportions designated CM60 and M60 were designed with the same water-cement ratio and sand-cement ratio, but with 50% (CM60) and 0% (M60) of the coarse aggregate. M60 is similar to the mix proportion of the mortar generally used for pre-pumping in placing of concrete.

Table 2 Mix proportions

Symbol	W/C (%)	s/a (%)	Unit content (kg/m^3)				
			W	C	S	G	Admixture
C30	30	37.6	167	557	604	1,030	2.785
C45	45	43.1		371	759		0.742
C60	60	45.5		278	837		0.556
CM60		69	223	371	1,114	515	0.742
M60		100	292	486	1,458	0	0

The materials are ordinary portland cement (produced by company N; specific gravity: 3.15 g/ cm^3; specific surface area: 3,260cm^2/g), river sand from the Fuji River (specific gravity: 2.63; absorption: 2.01%; fineness modulus: 2.75), and crushed sandstone from the Ryouzin area (specific gravity: 2.70; maximum size: 20mm; absorption: 0.51%, fineness modulus: 6.66). An AE-water reducing agent (produced by company F; oxycarboxylic acid) was used for concretes with water-cement ratios of 45% and 60%, and superplasticizer (company F; polycarboxylic acid) for concrete with a water-cement ratio of 30%.

2.4 Mixing procedure and curing

Concrete batches were mixed in a vertical-shaft (pan-type) mixer. Batches of 0.1 m^3 a batch were mixed continuously twice and the both were then mixed each other sufficiently in a vessel. The properties of the fresh-mixed concrete were then measured and the molds were filled.
All specimens were covered with a wet hemp cloth mat about 10 hours after placing to ensure wet curing until demolding. Contact-tips were pasted onto the uni-axially restrained specimens and free-shrinkage specimens when drying began. All specimens were then kept in a room at constant temperature and humidity: 20.5 ± 1.5℃ and 62 ± 5% RH.

3. RESULTS AND DISCUSSION

3.1 Physical properties

The measured physical properties of each concrete mix are presented in Table 3. Though the target slump value for all mixes was 8 ±2.5 cm, the concrete mix with a water-cement ratio of 30% (and containing the superplasticizer) had higher slump, as did the concrete with less coarse aggregate.

Though the air content was lower, at about 2.0%, in mortar mixes (M60) as a result of not using the AE-water reducing agent, the air content of all other mixes was 4.5 ± 1.5%. Mortar mixes also exhibited higher compressive strength as compared with concrete mixes at the same water-cement ratio, but because of the lower air content, and they had a lower Young's modulus and splitting tensile strength than concrete mixes of the same compressive strength.

Splitting tensile strength and Young's modulus at the age when drying started and at the age when cracking

Table 3 Results of physical properties tests

Experiment No.	Symbol of Mix proportion	Fresh: Slump (cm)	Fresh: Air content (%)	Fresh: Temp. of concrete (℃)	Fresh: Initial setting (h - m)	At start of drying (wet curing): Age (day)	At start of drying (wet curing): Compressive strength (N/mm^2)	At start of drying (wet curing): Young's modulus ($\times 10^4 N/mm^2$)	At start of drying (wet curing): Tensile strength (N/mm^2)	At age of 28 days (water curing): Compressive strength (N/mm^2)	At age of 28 days (water curing): Young's modulus ($\times 10^4 N/mm^2$)
1	C30	14.5	4.4	24.2	5 - 52	7	56.4	3.30	4.10	56.5	3.71
2	C45	10.0	4.6	21.2	5 - 25	7	33.6	2.93	2.78	43.0	3.40
3	C60	8.5	4.8	20.0	6 - 44	1	6.35	1.26	0.70	36.8	2.89
4		9.0	4.2	22.4	6 - 12	7	22.9	2.45	2.39	32.5	2.95
5		6.0	5.3	22.5	5 - 34	7	26.3	2.57	2.31	35.7	3.18
6		9.5	4.8	21.3	6 - 14	7	19.9	2.45	2.31	32.5	2.95
7		8.0	4.7	20.5	6 - 55	(7)	24.7	2.64	2.84	37.1	3.09
8	CM60	21.0	5.5	21.0	6 - 26	7	23.6	2.13	2.06	32.4	2.40
9	M60	22.0	2.1	21.1	6 - 57	7	26.6	1.93	2.02	40.1	2.30
10		23.0	1.9	19.8	7 - 52	7	24.6	1.96	2.05	39.8	2.29
11		21.5	1.7	20.0	7 - 40	7	24.0	1.90	1.86	40.2	2.34

Experiment No.	Symbol of Mix proportion	At age of 28 days (air curing): Compressive strength (N/mm^2)	At age of 28 days (air curing): Young's modulus ($\times 10^4 N/mm^2$)	At age of cracking firstly (air curing): Age (day)	At age of cracking firstly (air curing): Compressive strength (N/mm^2)	At age of cracking firstly (air curing): Young's modulus ($\times 10^4 N/mm^2$)	At age of cracking firstly (air curing): Tensile strength (N/mm^2)	At the age of cracking lastly (air curing): Age (day)	At the age of cracking lastly (air curing): Compressive strength (N/mm^2)	At the age of cracking lastly (air curing): Young's modulus ($\times 10^4 N/mm^2$)	At the age of cracking lastly (air curing): Tensile strength (N/mm^2)
1	C30	52.8	3.37	17	61.6	3.40	4.27	20	63.0	3.43	4.19
2	C45	47.9	3.01	18	42.6	2.96	3.08	24	45.1	2.96	3.06
3	C60	22.3	2.35	14	22.9	2.21	1.85	18	22.8	2.30	1.67
4		32.7	2.77	16	26.8	2.77	2.39	32	32.1	2.64	2.49
5		37.3	2.91	21	33.8	2.63	2.59	45	35.9	2.73	2.95
6		33.0	2.72	47	35.3	2.78	2.60	81	33.9	2.58	3.15
7		35.7	2.82	46	41.8	2.87	3.15	57	41.4	2.70	3.16
8	CM60	34.0	2.20	23	32.1	2.23	2.03	27	33.0	2.19	2.04
9	M60	43.1	2.19	10	31.0	1.99	2.30	14	34.6	2.12	2.18
10		39.9	2.09	15	34.6	2.05	2.66	19	37.3	2.10	2.07
11		40.7	2.13	16	34.9	2.08	2.25	20	36.8	2.13	2.22

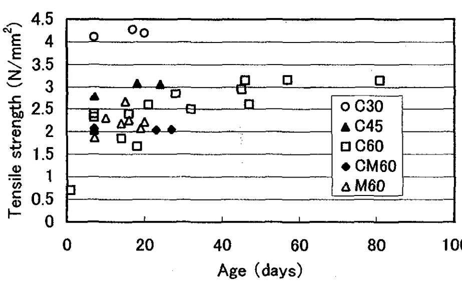

Fig.2 Results of tensile strength

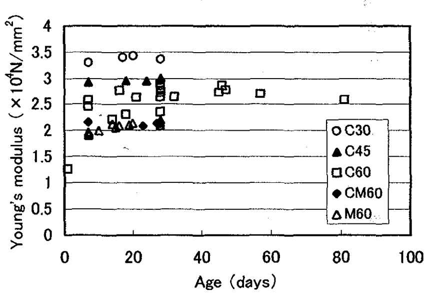

Fig.3 Results of Young's modulus

occurred, are given in Figs.2 and 3, respectively. Here, all specimens were cured in wet conditions until the start of drying, and thereafter exposed to drying conditions. The figures indicate that both splitting tensile strength and Young's modulus vary with mix proportion, and that development was slightly less after the age of 7 days. An empirical formula for Young's modulus in the case of each mix, taken from Fig.3, is given in Table 4.

Table 4 Empirical formulas for Young's modulus, $E=10000 \times x/(a+b \times x)$

	a	b
C30	0.0842	0.290
C45	0.0782	0.331
C60	0.401	0.361
CM60	0.264	0.463
M60	0.479	0.450

3.2 Age at cracking

A penetrating crack was observed in all restrained specimens, and the age at cracking ranged from 9.4 days to 80.4 days (or 2.4 to 73.4 drying days). The results for restrained shrinkage cracking test in all specimens are presented in Table 5. The age at which penetrating cracks were observed is plotted in Fig.4. These results indicate that the variation in cracking age generally increases as the age at cracking increases for the same experimental conditions. Taking into consideration on the age at cracking for every experimental parameter, following results are obtained.

Table 5 Results of restrained shrinkage cracking test

Experiment / Specimen		Age at cracking (days)	Location of crack	Pattern of fracture *	Just before cracking				At penetrating cracking		
					Age of measurement (days)	Free shrinkage strain ($\times 10^{-6}$)	Restrained shrinkage strain ($\times 10^{-6}$)	Restrainred tensile strain ($\times 10^{-6}$)	Shrinkage stress (N/mm^2)	Tensile strength (N/mm^2)	Ratio of shrinkage stress - tensile sterngth
No.1	1	17.3	5	Mini. shrinkage	16.2	-403	-193	210	2.54	4.26	0.60
	2	18.9	3	Mini. shrinkage	18.0	-443	-215	228	2.65	4.21	0.63
	3	18.3	3	Mini. shrinkage	18.0	-443	-198	245	2.52	4.23	0.60
	4	19.7	5	Mini. shrinkage	18.0	-443	-200	243	2.61	4.19	0.62
	5	16.9	3	Expansion	16.2	-403	-183	220	2.56	4.27	0.60
	Ave.	18.2						229			0.61
No.2	1	17.6	1	Mini. shrinkage	17.2	-335	-144	191	1.87	3.08	0.61
	2	19.1	4	Mini. shrinkage	18.0	-341	-143	198	1.87	3.07	0.61
	3	19.3	2	Mini. shrinkage	18.0	-341	-151	190	1.60	3.07	0.52
	4	23.2	4	Mini. shrinkage	22.3	-379	-172	207	2.05	3.06	0.67
	5	18.8	2	Mini. shrinkage	18.0	-341	-131	210	1.88	3.08	0.61
	Ave.	19.6						199			0.60
No.3	1	14.2	4	Mini. shrinkage	12.0	-248	-92	156	1.11	1.85	0.60
	2	18.1	1	Without Indi.	17.0	-297	-129	168	1.69	1.69	1.00
	3	18.7	4	Without Indi.	17.0	-297	-118	179	1.73	1.67	1.04
	4	17.7	1	Mini. shrinkage	17.0	-297	-102	195	1.49	1.71	0.87
	5	17.8	3	Mini. shrinkage	17.0	-297	-111	186	1.36	1.70	0.80
	Ave.	17.3						177			0.86
No.4	1	30.5	2	Mini. shrinkage	30.0	-387	-136	251	2.17	2.49	0.87
	2	30.8	4	Mini. shrinkage	30.0	-387	-147	240	2.20	2.49	0.88
	3	16.0	2	Mini. shrinkage	16.0	-242	-82	160	1.50	2.39	0.63
	4	20.3	4	Mini. shrinkage	20.3	-291	-89	202	1.69	2.42	0.70
	5	26.3	4	Mini. shrinkage	25.3	-334	-97	237	2.05	2.46	0.83
	Ave.	24.8						218			0.78
No.5	1	32.4	4	Expansion	31.0	-399	-210	189	2.23	2.77	0.80
	2	36.7	2	Without Indi.	35.1	-435	-190	245	2.43	2.84	0.86
	3	34.4	2	Mini. shrinkage	33.2	-418	-182	236	2.28	2.80	0.81
	4	20.8	2	Mini. shrinkage	19.2	-283	-118	165	1.84	2.59	0.71
	5	44.1	3	Mini. shrinkage	42.2	-467	-219	248	2.53	2.95	0.86
	Ave.	33.7						217			0.81
No.6	1	51.0	2	Mini. shrinkage	50.0	-502	-282	220	2.27	2.68	0.85
	2	46.3	4	Without Indi.	45.0	-482	-283	199	2.27	2.60	0.87
	3	80.4	4	Mini. shrinkage	80.0	-585	-273	312	2.70	3.15	0.86
	4	69.1	1	Mini. shrinkage	66.2	-569	-315	254	2.50	2.97	0.84
	5	59.8	2	Mini. shrinkage	59.0	-543	-260	283	2.48	2.82	0.88
	Ave.	61.3						254			0.86
No.7	1	52.9	4	Expansion	51.0	-403	-185	218	2.31	3.15	0.73
	2	56.3	4	Mini. shrinkage	55.3	-453	-190	263	2.35	3.15	0.75
	3	56.9	3	Without Indi.	55.3	-453	-196	257	2.50	3.15	0.79
	4	57.0	2	Mini. shrinkage	55.3	-453	-180	273	2.53	3.16	0.80
	5	45.5	2	Without Indi.	44.0	-374	-179	195	1.98	3.15	0.63
	Ave.	53.7						241			0.74
No.8	1	26.3	5	Mini. shrinkage	25.1	-407	-174	233	1.69	2.04	0.83
	2	25.6	2	Mini. shrinkage	25.1	-407	-182	225	1.73	2.04	0.85
	3	23.1	5	Mini. shrinkage	23.0	-356	-130	226	1.38	2.03	0.68
	4	23.3	5	Mini. shrinkage	23.0	-356	-165	191	1.77	2.03	0.87
	5	23.9	2	Mini. shrinkage	23.0	-356	-140	216	1.79	2.03	0.88
	Ave.	24.4						218			0.82
No.9	1	10.3	2	Without Indi.	10.0	-141	-55	86	1.35	2.28	0.59
	2	10.0	2	Mini. shrinkage	9.1	-119	-53	66	0.63	2.28	0.28
	3	9.4	4	Mini. shrinkage	9.1	-119	-40	79	1.09	2.30	0.48
	4	13.7	2	Without Indi.	13.3	-228	-55	173	1.85	2.18	0.85
	5	10.8	4	Mini. shrinkage	8.0	-69	-32	37	0.70	2.26	0.31
	Ave.	10.8						88			0.50
No.10	1	15.3	1	Mini. shrinkage	15.2	-283	-114	169	1.71	2.56	0.67
	2	18.4	4	Mini. shrinkage	18.2	-322	-105	217	1.99	2.07	0.96
	3	16.5	4	Mini. shrinkage	16.0	-286	-126	160	1.72	2.37	0.73
	4	14.6	4	Mini. shrinkage	14.2	-267	-94	173	1.56	2.66	0.59
	5	18.2	3	Mini. shrinkage	18.2	-322	-122	200	1.83	2.10	0.87
	Ave.	16.6						184			0.76
No.11	1	16.1	4	Mini. shrinkage	16.1	-319	-149	170	1.58	2.25	0.70
	2	17.9	3	Mini. shrinkage	17.2	-346	-185	161	1.59	2.24	0.71
	3	16.6	3	Mini. shrinkage	16.1	-319	-155	164	1.56	2.25	0.69
	4	19.9	2	Expansion	19.2	-379	-217	162	1.85	2.22	0.83
	5	18.6	3	Expansion	18.0	-348	-195	153	1.74	2.23	0.78
	Ave.	17.8						162			0.74

* Mini. shrinkage: Cracks occur at the point showed minimum shrinkage strain.
Expansion: Cracks occur at the point showed expansive strain before cracking.
Without indi.: Cracks occur without sign of cracking.

The time until cracking (averaged over the five specimens) was 18.2, 19.6, and 33.7 days in the case of water-cement ratios of 30%, 45%, and 60% (experiment Nos.1, 2, and 5), respectively. This indicates that cracks occurred at an earlier age as the water-cement ratio decreased. According to a report by Makizumi et al. [11] on the cracking age for water-cement ratios ranging from 40% to 60% and a report by the Society for the Research of Cracking [12] for water-cement ratios from 50% to 70%, cracking occurs at almost the same age regardless of water-cement ratio. On the other hand, in a report by Hisaka et al. [13] on water-cement ratios ranging from 25% to 60% and one by Yasuda et al. [14] for ratios ranging from 27% to 60%, it is indicated that cracks occur earlier when the water-cement ratio is reduced. Taking into consideration inclusive of our experimental results, it can be seen that cracking occurs earlier when the water-cement ratio is lower than 45%. It can be assumed that this tendency is generally due to greater free-shrinkage strain during wet curing (higher autogenous shrinkage) and lower relaxation of stress due to concrete creep [14] [15].

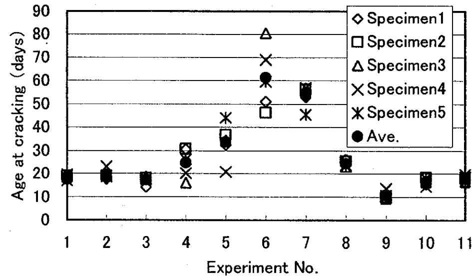

Fig.4 Ages at cracking

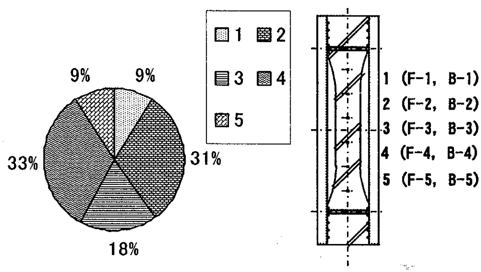

Fig.5 Location of cracking

The time until cracking (averaged over the five specimens) was 17.3, 33.7, and 53.7 days (or 16.3, 26.7, and 25.7 drying days) when drying started at 1, 7, and 28 days (experiment Nos.3, 5, and 7), respectively. These results indicate that penetrating cracks occur earlier when the initial moisture curing period is extremely short. Although in the report by Makizumi et al. [11] on cracking age when drying starts at 2, 3, 7, 14, and 28 days and in the report by Society for the Research of Cracking [15] for drying starts at 2, 3, and 7 days it is observed that cracking age does not clearly correlate with age at which drying starts, it can be seen in these results that cracks occur earlier when drying starts at 2 days. Therefore, taking into consideration inclusive of our experimental results, it can be seen that the time until cracking become earlier in the case of shorter wet curing period of 2 days or less.

The time until cracking (averaged over the five specimens) was 24.8, 33.7, and 61.3 days when the sectional area of the restraint frame was 1,019, 697, and 496 mm^2 (experiment Nos.4, 5, and 6), respectively. These results indicate that penetrating cracks occur earlier when the degree of restraint is higher. This tendency is similar to that in Makizumi et al. [11] and Suzuki et al. [16] report. Although the results also indicate that penetrating cracks in mortar mixes also occur earlier slightly as the restraint is increased (experiment Nos.9, 10, and 11), the cracks occurred relatively earlier as compared with concrete mixes and there was no significance in the correlation with sectional area of the restraint frame.

Finally, the time until cracking (averaged over the five specimens) was 61.3, 24.4, and 17.8 days in the case of coarse aggregate amounts of 1,030, 515, and 0 kg/m^3 (experiment Nos.6, 8, and 11), respectively. These results indicate that penetrating cracks of concrete occur earlier as the amount of coarse aggregate is reduced; that is, as the mortar volume increases.

3.3 Location of cracks

In all cases, the penetrating cracks observed in restrained specimens occurred within the region where strain measurements were made (in the middle of specimen: 500 mm span). The distribution of crack location is presented in Fig.5 based on the strain measurement locations (numbered 1 - 5 from the top). Though the penetrating cracks in all restrained specimens occurred within the straight part (2 - 4) in about 82% of specimens, they occurred in the tapered area in the remaining 18% of cases (1, 5).

3.4 Relationship between strains

The relationship between the free-shrinkage strain of the free-shrinkage specimen, and restrained shrinkage strain and/or restrained tensile strain of uni-axially restrained specimens is shown in Fig.6. Equations (1) to (4) show the relationships between elastic strain and creep strain of the concrete due to forces imposed by the restraint frame. Here, a minus sign in the strain means shrinkage and a plus sign means expansion.

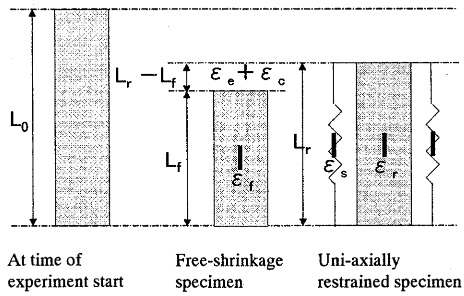

Fig.6 Relation between strains

$$\varepsilon_f = (L_f - L_0)/L_0 \tag{1}$$
$$\varepsilon_r = (L_r - L_0)/L_0 \tag{2}$$
$$\varepsilon_e + \varepsilon_c = (L_r - L_f)/L_0 \tag{3}$$
$$\varepsilon_r = \varepsilon_e + \varepsilon_c + \varepsilon_f \tag{4}$$
$$K = -(\varepsilon_e + \varepsilon_c)/\varepsilon_f \tag{5}$$

Where ε_f is Free-shrinkage strain, ε_r is restrained shrinkage strain, and $\varepsilon_e + \varepsilon_c$ is restrained tensile strain. And ε_e is elastic strain, ε_c is creep strain, and K is actual degree of restraint.

Further, relationships obtained under the conditions of balance of forces between the restraint frame and the concrete in uni-axially restrained specimens and of agreement of strain are presented in Equations (6) and (7). Equation (8) is calculated from the above equations, and Equation (4) can then be rewritten as Equation (9) on the assumption that the increase in stress in a time increment (Δt) occurs at the mid-point of Δt and that elastic strain and creep strain occurs due to this stress. Equation (10) is then obtained from Equations (8) and (9), and shrinkage stress can be calculated through successive analysis. Here, a plus sign means tensile stress.

$$\varepsilon_s = -\varepsilon_e E_c A_c / E_s A_s \tag{6}$$
$$\varepsilon_s = \varepsilon_r \tag{7}$$
$$\varepsilon_{r,i} = -\sigma_{c,i} A_c / E_s A_s \tag{8}$$
$$\varepsilon_{r,i} = \sum_{j=1}^{i} \left\{ (\sigma_{c,j} - \sigma_{c,j-1})(1 + \phi_{i,j-0.5}) / E_{c,j-0.5} \right\} + \varepsilon_{f,i} \tag{9}$$
$$\begin{aligned} \sigma_{c,i} = {} & -1/\left(A_c / E_s A_s + (1 + \phi_{i,i-0.5})/E_{c,i-0.5}\right) \\ & \Big\{ \sum_{j=1}^{i-1} \left\{ (\sigma_{c,j} - \sigma_{c,j-1})(1 + \phi_{i,j-0.5}) / E_{c,j-0.5} \right\} - \\ & \sigma_{c,i-1}(1 + \phi_{i,i-0.5})/E_{c,i-0.5} + \varepsilon_{f,i} \Big\} \end{aligned} \tag{10}$$

Where ε_s is strain of restraint frame. E_s and A_s are Young's modulus and sectional area of restraint frame, respectively. E_c and A_c are Young's modulus and sectional area of concrete, respectively. $\sigma_{c,i}$ is shrinkage stress at age i and $\phi_{i,j}$ is creep coefficient at age i for stress acting at age j $(\varepsilon_c / \varepsilon_e)$.

3.5 Free-shrinkage strain

Example time-histories for concrete strain in free-shrinkage specimens (free-shrinkage strain) for each measuring

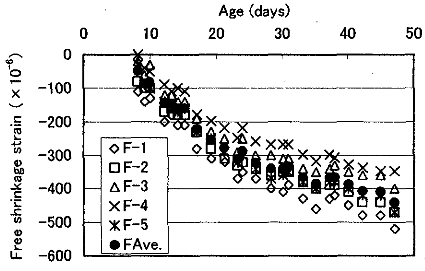

(a) Placing surface

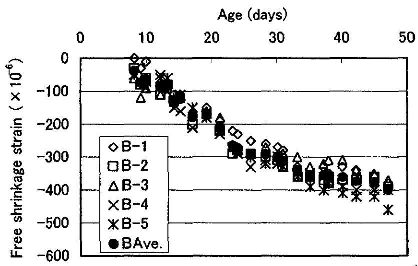

(b) Bottom side

Fig.7 Time histories of free-shrinkage strain for each measuring point (Experiment No.5, specimen No.2)

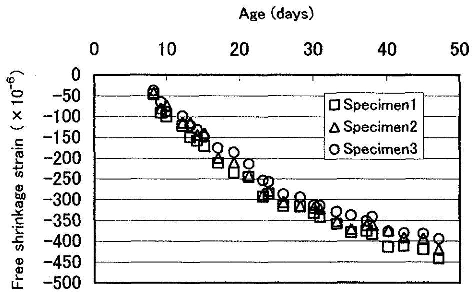

Fig. 8 Time histories of average free-shrinkage strain for 10 measuring points (Experiment No.5)

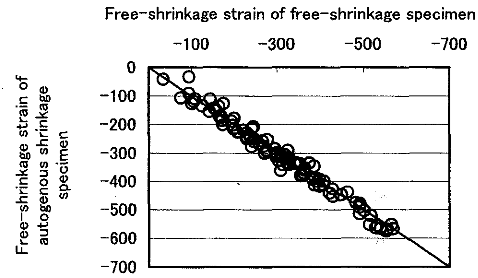

Fig.9 Difference in free-shrinkage strain among shapes of the specimens

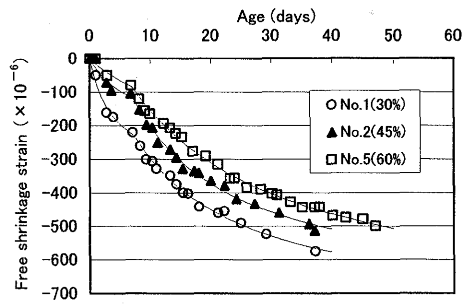

Fig.10 Time histories of free-shrinkage strain after placing (water-cement ratio)

point after drying are presented in Fig.7. Figure 7(a) shows values taken at the five points (F-1 - F-5 from the top) spaced 100 mm apart on placing surface, while Fig.7 (b) shows equivalent values for the bottom (B-1 - B-5 from the top). Since experiment No.5 is set up with conditions representing the mid-point of all the experimental factors considered in this research, the results for this case will be the focus of the discussion from here on. It is clear from these two figures that the free-shrinkage strain on the placing surface is in general greater than that at the bottom. Also, the concrete at all measuring points shrinks in almost the same breath in spite of variations in strain among measuring points.

Averaged time histories for free-shrinkage strain at the ten measuring points on the placing surface and on the bottom of each free-shrinkage specimen are shown in Fig.8. It is clear from this figure that variations in free-shrinkage strain among the three free-shrinkage specimens were very small and, as above, no variations among measuring points are apparent.

The free-shrinkage strain of specimens measured for free-shrinkage specimen and autogenous shrinkage specimen is compared in Fig.9. Though the specimens differed in measurement length (300 mm and 500 mm), and in the shape of the specimen ends, it is clear from this figure that the strains are almost equivalent. It is conceivable that the free-shrinkage strain of an autogenous shrinkage specimen could be substituted for that of a free-shrinkage specimen.

Example time histories of free-shrinkage strain after placing for various water-cement ratios are presented in

Table 6 Constants in empirical formula for each free-shrinkage strain

Experiment No.	y=-x/(a+b*x)		y=c-(x-t)/(d+e*(x-t))			
	a	b	t	c	d	e
1	11697	2763.8	7.05	-0.000221	32840	1812
2	31179	4206	6.76	-0.000105	27623	1648
3	37359	1132.6	-	-	-	-
4	66697	5913.5	6.94	-6.28E-05	31541	1841
5	60886	3234.4	6.83	-8.05E-05	38083	1461
6	102254	3974.9	6.88	-5.33E-05	41707	1271
7	58770	5613.1	28.20	-0.000118	28145	2060
8	3581094	448216	7.45	-3.06E-05	32909	898
9	66341	6664.8	7.40	-5.72E-05	29890	825
10	854417	58027	7.26	-1.44E-05	21018	1070
11	71300	10419	7.30	-5.11E-05	25721	884

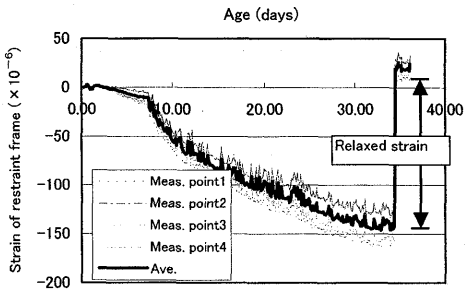

Fig.11 Time histories of strain in restraint frame for each gauge (Experiment No.5, specimen No.3)

Fig.10. Here, the free-shrinkage strain is expressed as the sum of the free-shrinkage strain for an autogenous shrinkage specimen under wet curing and that for a free-shrinkage specimen after drying. This is because the free-shrinkage strain for both specimens (which have the same sectional area of concrete) did not differ in spite of the different specimen shape. These strains were averaged over three specimens and the approximate curve is plotted in this figure. Empirical constants for equations of the form $y = -x/(a + b \times x)$ before drying and $y = c - (x - t)/(d + e \times (x - t))$ after drying for each free-shrinkage strain are presented in Table 6.

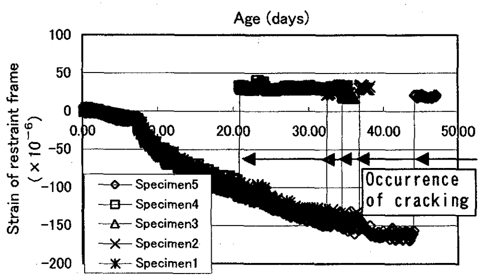

Fig.12 Time histories of averaged strain in restraint frame (Experiment No.5)

It is clear from Fig.10 that the free-shrinkage strain is larger with a water-cement ratio of 30% than with a water-cement ratio of 45% or 60%. Looking more closely, the free-shrinkage strain up to 7 days is larger in the case of a 30% ratio (experiment No.1), whereas after 7 days the changes in free-shrinkage strain are similar whatever the water-cement ratio.

3.6 Strain of restraint frame

Time histories of restraint frame strain for one uni-axially restrained specimen as measured at four strain gauges are presented in Fig.11. It is clear from this figure that a shrinkage strain of about 15 $\times$ 10^{-6} occurred during wet curing up to the age of 7 days, and thereafter shrinkage strain increased uniformly with drying age. The time history at each measuring point varied slightly.

Time histories of averaged shrinkage strain for the four gauges in the restraint frame (averaged over the four gauges) for the same experimental conditions are shown in Fig.12. It is clear from this figure that variations in shrinkage strain among the five specimens are smaller than the variations among the four measuring points. The age at cracking varied between about 21 and 44 days, and significant variation in age at cracking are indicated among the five specimens in spite of the fact that the time histories of averaged restraint frame strain are similar. It can be assumed that the distribution of strain over the cross section and along the axis of the concrete, as well as the varying number of internal defects in the concrete, result in the spread in cracking age.

Figure 12 also shows that strain in the restraint frame reversed and became an expansion when a penetrating crack formed, though expansion strain was not almost observed just after initial setting. This tendency was recognized in all specimens with various levels. In work by other researchers on concrete specimens with embedded reinforcement and a water-cement ratio of 24 percent [17], it has been reported that shrinkage strain in the reinforcement begins to occur from the age of 14 hours and stress is delayed as compared with the development of strain, even though concrete begins to undergo autogenous shrinkage immediately after initial setting (at about 9 hours). In our experiment using uni-axially restrained specimens, it is conceivable that the concrete and the restraint frame were in some way fixed to each other when the expansion occurred as a result of wet curing and heat of hydration after initial setting. If this happened, and the expansion strain would have been added to the strain in restraint frame that returned at the time of cracking. Therefore, it was guessed that agreement of strain did not come to existence in a strict sense during early age.

3.7 Restrained shrinkage strain

Example time histories for the strain of concrete in a restrained specimen at the ten measuring points after drying are presented in Fig.13. It is clear from this figure that each measuring point had a different time history as that shrank in the almost same breath, as that did not shrink from early drying period, and as that stopped shrinking on the way of drying, and the variation in strain among measuring points was bigger. This tendency shown various strains among measuring points is recognized in all specimens and the phenomenon being not able to shrink in the same breath grew stronger under restraint due to the restraint frame.

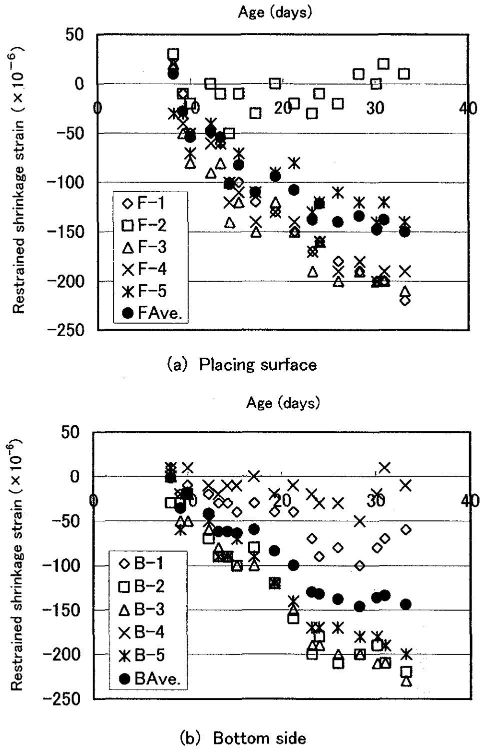

Fig.13 Time histories of restrained shrinkage strain for 10 measuring points (Experiment No.5, specimen No.3)

The penetrating crack formed at the second measuring point from the top in this specimen, though the concrete did not almost shrink at measuring point on placing surface (F-2) as shown in this figure and shrank in the almost same breath at the measuring point on the bottom (B-2). In about 76% of all specimens, the penetrating crack formed at the measuring point that registered expansion from an early age and/or the measuring point indicating the minimum shrinkage strain (mini. shrinkage shown in Table 5). Cracks were observed at many measuring points being not able to shrink and at acting higher tensile strain due to higher shrinkage strain near the cracking point. As for the other cases, 9% of specimens suffered a penetrating crack after exhibiting expansion strain immediately before cracking (expansion shown in Table 5) and 15% suddenly suffered a penetrating crack without expansion after shrinking in the same breath (without indi. shown in Table 5). It is necessary to take into account the time interval between time of the measurement just prior to cracking and the actual time of cracking, since concrete strain was measured at intervals of one or two days.

Concrete strain in just measuring point of cracking rapidly switched to the expansion side and strain around the crack moved in the shrinkage direction at the time when the penetrating crack occurred in the case of specimens under restraint. The area in which strain moved to the shrinkage side is the area enclosed by the measuring points, and it can be thought that the strain at all measuring point is released from restraint when the crack occurs. That is to say, the area of strain release is the area influencing cracking.

The difference between strain in measuring point shrinking in the same breath and strain in measuring point not shrinking increased with increasing drying time in all specimens, as shown in Fig.13. According to a past report [20], a crack occurs immediately after an increase in tensile strain at the cracking point. On the other hand, tensile strain around the cracking point tends to relax when a uni-axial tensile stress acts on a prism specimen. It is clear from our experiments that there is no matching tendency in the time history of strain at the cracking point. This is because cracking point varied in measuring point as showing minimum shrinkage, as showing expansion strain immediately before cracking, and as showing sudden occurrence of penetrating crack without expansion after shrinking in the same breath as mentioned above.

One set of histories (experiment No.5) of restrained shrinkage strain averaged over 10 measuring points is presented in Fig.14. It is clear from this figure that the variation in concrete strain among uni-axially restrained specimens is bigger than that among free-shrinkage specimens, and is easily appeared as compared with that of restraint frame, though concrete shrinks as a general tendency. It is conceivable that the variation in restrained shrinkage strain among measuring points, as shown in Fig.13, influences that among uni-axially restrained specimens and that this variation in restrained shrinkage strain among specimens causes the difference in age at cracking even under the same experimental conditions.

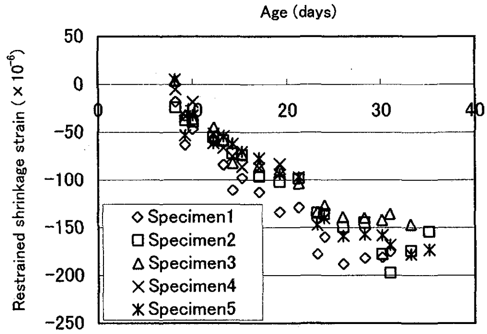

Fig.14 Time histories of average restrained shrinkage strain for 10 measuring points (Experiment No.5)

The relationship between restrained shrinkage strain of concrete and strain of the restraint frame at the same time is plotted in Fig.15. It is quite clear from this figure that the strain of the restraint frame is smaller than the restrained shrinkage strain. According to a report on differences in concrete strain and/or restraint frame strain as measured using various methods, the values given by contact-type strain gauges are bigger than that of wire strain gauges once the strain reaches about 50 $\times$ 10^{-6}, with strain gauge reading being about 70% - 75% those of contact-type strain gauges [15]. It is conceivable that both concrete and restraint frame shrink equally and that the strain equalizes once drying starts, taking the difference in measuring method into consideration, because the strain of the restraint frame measured by wire strain gauges indicates about 80% of the concrete strain measured by contact-type strain gauges.

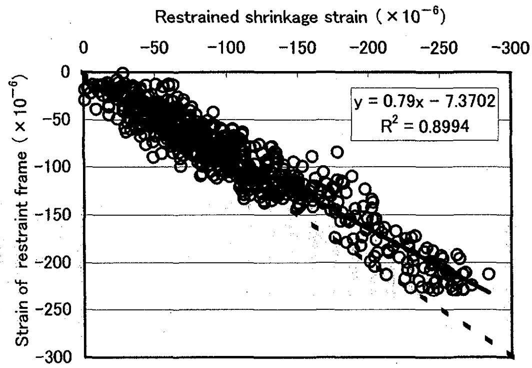

Fig.15 Relationship between restrained shrinkage and strain of restraint frame

3.8 Restrained tensile strain

Time histories for restrained tensile strain with each experimental factor as a parameter are presented in Fig.16 (a) - (e). Here, the approximate curve of restrained tensile strain is plotted as a solid line. Restrained tensile strain is defined as the difference between the concrete strain measured for a free-shrinkage specimen and the concrete strain measured for a restrained specimen; that is, the strain resulting from the tensile stress imposed by the restraint frame. The strain values in these figures are averages over the five uni-axially restrained specimens. The restrained tensile strain occurring during wet curing was calculated using Equation (11) on the assumption that degree of restraint during wet curing was the same with that during the drying period, because measurements of restrained shrinkage strain began only in the drying stage.

$$\varepsilon_e + \varepsilon_c = -K \times \varepsilon_{f,wet} + (\varepsilon_e + \varepsilon_c)_{dry} \tag{11}$$

Where, $\varepsilon_{f,wet}$ is free-shrinkage strain during wet curing and $(\varepsilon_e + \varepsilon_c)_{dry}$ is restrained tensile strain during drying period.

Figure 16(a) indicates the influence of water-cement ratio on restrained tensile strain, 16(b) indicates the influence of age when drying started, 16(c) indicates the influence of amount of coarse aggregate, and 16(d) and 16(e) indicate the influence of sectional area of the restraint frame, respectively. Free-shrinkage strain is the value measured just before cracking and restrained tensile strain was calculated using values of restrained shrinkage

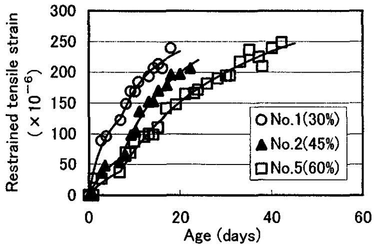

(a) Influence of water-cement ratio

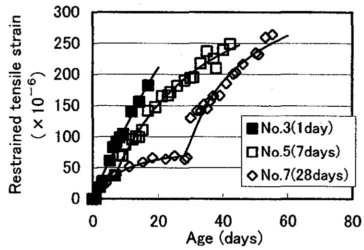

(b) Influence of age at which drying starts

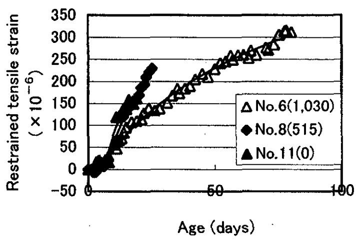

(c) Influence of amount of coarse aggregate

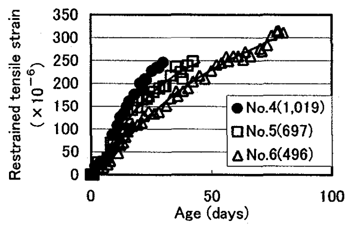

(d) Influence of sectional area of restraint frame (Mix proportion: C)

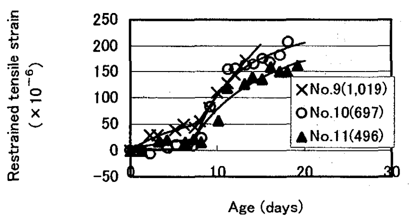

(e) Influence of sectional area of restraint frame (Mix proportion: M)

Fig.16 Time histories of restrained tensile strain

strain presented in Table 5.

Cracking occurred earlier with a lower water-cement ratio, earlier drying, less coarse aggregate, and bigger sectional area of restraint frame. It is also very clear from these figures that the restrained tensile strain was higher at the same age and time history of restrained tensile strain was plotted in upper side in this figure in the case of experimental condition which cracking occurred earlier. These results demonstrate that the age at cracking become earlier in the case of experimental condition with higher restrained tensile strain and influence of various factors on occurrence of cracks can be judged by restrained tensile strain.

4. CRITICAL CRACKING LIMIT

Two criteria have been considered as possible indexes of the critical cracking limit: the point when restrained tensile strain exceeds tensile strain capacity (restrained tensile strain at the time of cracking); and the point when shrinkage stress exceeds tensile strength. The applicability of these criteria is investigated in this section.

4.1 Tensile strain capacity

Data from past investigations and also that obtained in our experiments are shown in Fig.17 in the form of a plot of drying days until cracking against tensile strain capacity. Only past data for specimens matching the restraint conditions used in our experiment is selected. Tensile strain capacity from our experiment is also indicated in terms of post-drying strain. The length over which strain was measured in the past results was 200 – 300mm, while it was 500 mm (and stated strain values are the average over this length) in our experiments.

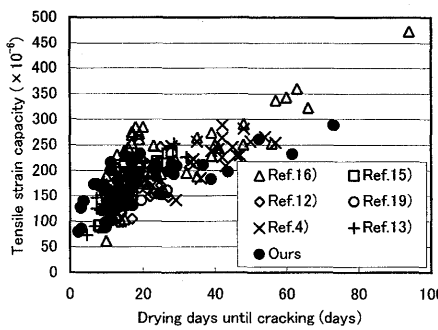

Fig.17 Tensile strain capacity vs drying days until cracking

First, it is clear that the data obtained in our experiments fall roughly among the past data, and the more drying days until cracking, the higher the tensile strain capacity. Though it has not been reported a number of times that tensile strain capacity increases with increasing drying time until cracking [12], a similar tendency is certainly evident in this figure.

The relationship between age at cracking and the tensile strain capacity at the cracking point (one measuring point; strain measured over 100 mm on one side) is plotted in Fig.18 (a) and that between age and tensile strain capacity averaged over all measuring points (ten points) is plotted in Fig.18 (b). While it is clear from Fig.18 (a) that tensile strain capacity at the cracking point does not correlate with age at cracking, Fig.18 (b) shows that there is clearly a relationship with averaged tensile strain capacity, though the measured strain values show a slight variance. The rise in tensile strain capacity with increasing time until cracking can be explained as a reason why part of elastic strain become higher because development of Young's modulus is lower than that of shrinkage stress and part of creep strain become higher because minute cracks in concrete is occurred by shrinkage stress. While minute cracks that develop in the vicinity of the interface between mortar and coarse aggregate as a result of early-age shrinkage stress may later become penetrating cracks because of the low bond strength between mortar and coarse aggregate. On the other hand, the occurrence of minute cracks does not immediately result in penetrating cracking because more strain can be accumulated in concrete in the case of exposing to drying after long-term curing and there is greater bond strength between mortar and coarse aggregate.

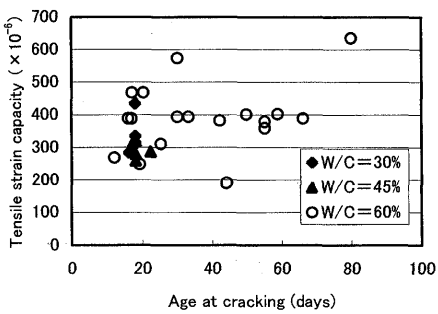

(a) Tensile strain capacity at cracking point
(measuring length of strain = 100mm, one side)

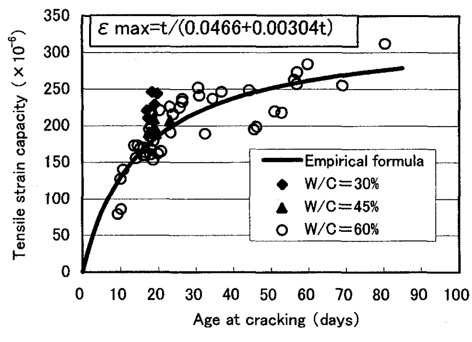

(b) Average tensile strain capacity over all measuring points
(measuring length of strain = 500mm, both sides)

Fig.18 Age at cracking vs tensile strain capacity

This makes clear that tensile strain capacity at the point of cracking does not govern cracking and is unsuitable as a cracking index. This is because the strain at any one measuring point, including the cracking point, is influenced by strain in the neighboring concrete, and that strain indicates a complex time history that depends on distance from the measuring point. On the other hand, it can be concluded that averaged tensile strain capacity is suitable as a critical index for use in predicting the time of cracking. This is because it includes the balance of strain in the area around the cracking point as a whole.

The relationship shown in Fig.18 (b) between averaged tensile strain capacity and age at cracking (represented from here on as a curve and drawn as a solid bold line) is shown once again for reference in Fig.19 along with the experimental time histories of restrained tensile strain taken from Fig.16. This figure once again shows that cracks occur when the restrained tensile strain reaches the curve of tensile strain capacity, though this is quite natural as the tensile strain capacity curve is essentially taken from the experimental data. However, it was not known whether concrete, for example, a water-cement ratio of 30% (experiment No.1) ought to have a different curve of tensile strain capacity (i.e. if it fitted a different empirical formula) until age of 10 days, since restrained tensile strain exceeded curve of tensile strain capacity from earlier age.

4.2 Ratio of shrinkage stress to tensile strength

The relationship between age at cracking and shrinkage stress at that time is plotted in Fig.20. Here, the shrinkage stress was calculated using Equation (8). Remembering the equivalence of concrete strain and restraint frame strain at early age, it is clear that the difference in restraint frame strain between the points just before and just after cracking (known as the returned strain: restraint frame strain after post-crack relaxation, see Fig.11) is exactly the restraint frame strain at the time when cracking occurs, and this returned strain is adopted in place of the accumulated strain since the beginning of the experiment. The shrinkage stress correlates with age at cracking for all experimental cases, and a higher shrinkage stress is indicated in experimental cases where the water-cement ratio was 30% as compared with other cases.

The ratio of shrinkage stress to tensile strength (the shrinkage stress to tensile strength ratio) is presented for all specimens in Fig.21 (a). Here, tensile strength at the cracking age, as given in Table 5, was calculated by compensation with straight line from results of tensile strength tests performed when cracks were first observed in the five restrained specimen and last observed in those specimens (see Table 5). This figure clearly demonstrates that cracking occurred when the ratio of shrinkage stress to tensile strength was higher as compared with another experimental cases for the same age at cracking for cases where drying started at one day (experiment No.3) and/or where the mix was mortar only (experiments No.8 - 11). On the other hand, a lower ratio of shrinkage stress to tensile strength was indicated in the case of experiment when drying started at 28 days (experiment No.7). It can be conceivable that cracks occur when higher ratio of shrinkage stress to tensile strength is operated in the case of mix proportion with higher free-shrinkage strain at the earlier age and experiment with insufficient development of tensile strength due to the earlier starting age of drying (experiments No.3, No.8 - 11), on the other hand when lower ratio of shrinkage stress to tensile strength is operated in the case of experiment exposed to drying after sufficient development of tensile strength due to long wet curing (experiment No.7).

Figure 21(b) plots only data for specimens where drying started at 7 days with the exception of experimental cases

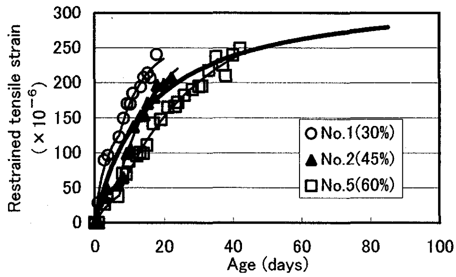

(a) Influence of water-cement ratio

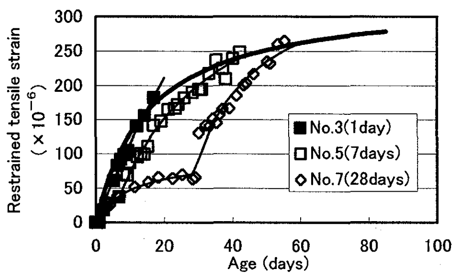

(b) Influence of age at which drying starts

Fig.19 Curves of tensile strain capacity

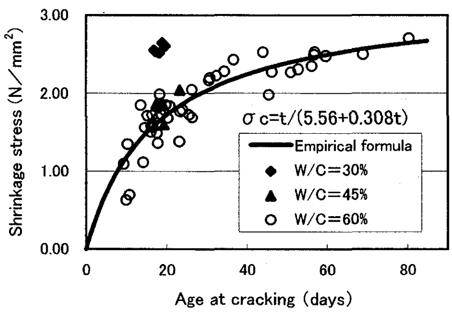

Fig.20 Age at cracking vs shrinkage stress

with different development of tensile strength (experiments No.3 and No.7 - 11) from Fig.21 (a). It is clear from this figure that the ratio of shrinkage stress to tensile strength increases with age at cracking until 40 days, and that cracking does not occur if the ratio of shrinkage stress to tensile strength does not exceed 85% of the tensile strength after the age of 40 days.

The occurrence of a penetrating crack in uni-axially restrained specimens may be viewed as a creep failure phenomenon after long-term loading due to gradually developing shrinkage stress (tensile stress). Generally speaking, where concrete is sufficiently hardened, creep failure occurs at an earlier age in the case of a higher ratio of stress to strength or after long-term loading in the case of a lower ratio of stress to strength. The creep limit is 75% - 85% of the strength, and creep failure does not occur if the ratio of stress to strength remains under 75% [21].

It is very clear from the figure that the creep limit was indicated 50% - 60% at the age of about 20 days and 85% after 40 days, though the specimen was subjected to gradually developing shrinkage stress in this experiment. It is conceivable that occurrence of minute cracks may immediately lead penetrating crack when the shrinkage stress equivalent to tensile strength ratio of 50% - 60% operates in concrete at earlier age. Creep limit become smaller at earlier age of cracking because pore structure and/or bond strength between mortar and coarse aggregate have not developed sufficiently. On the other hand, it is conceivable that occurrence of minute cracks may not lead penetrating crack at this moment because the shrinkage stress equivalent to tensile strength of only 20% - 30% operates in concrete at earlier age in the case of longer age at cracking and the ratio of shrinkage stress to tensile strength to develop from minute crack to penetrating crack become higher because bond strength between mortar and coarse aggregate smoothly develops.

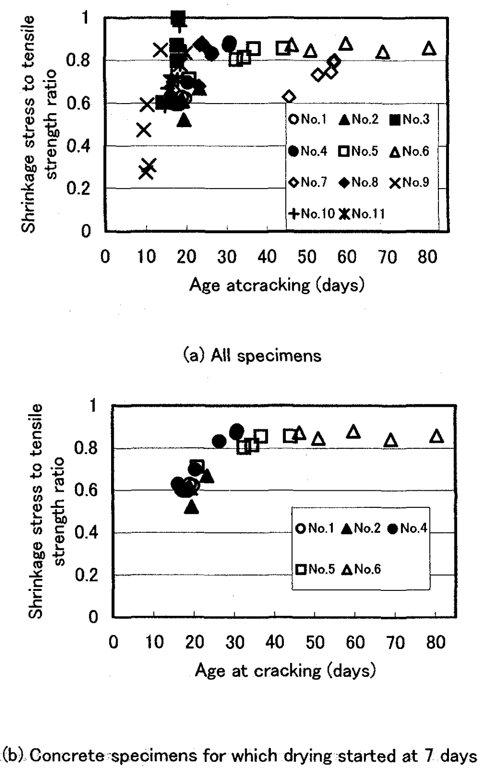

Fig.21 age at cracking vs shrinkage stress to tensile strength ratio

5. ANALYTICAL APPROACH

The shrinkage stress is calculated iteratively using Equation (10), and then the restrained tensile strain is calculated from the relationship between Equations (4) and (8). The resulting calculated time histories of restrained tensile strain are presented in Fig.22 among with experimental results (calculated values: solid line; measured values: marks). Here, the free-shrinkage strain (see Table 6), Young's modulus (see Table 4), and the sectional area of the concrete and restraint frame were taken from the experimental data as inputs, and the creep coefficient indicated in model code 1990, CEB - FIP was adopted and calculated using Equations (12) - (17). The time step was set at one day to ensure precision of analysis, though it has been reported that in the past that the results of analysis change little as the time step is varied from 2 to 10 days. Further, Young's modulus was modified to reflect the age of the concrete, because the model code makes use of Young's modulus at an age of 28 days.

Details of constant-setting are given in the model documentation.

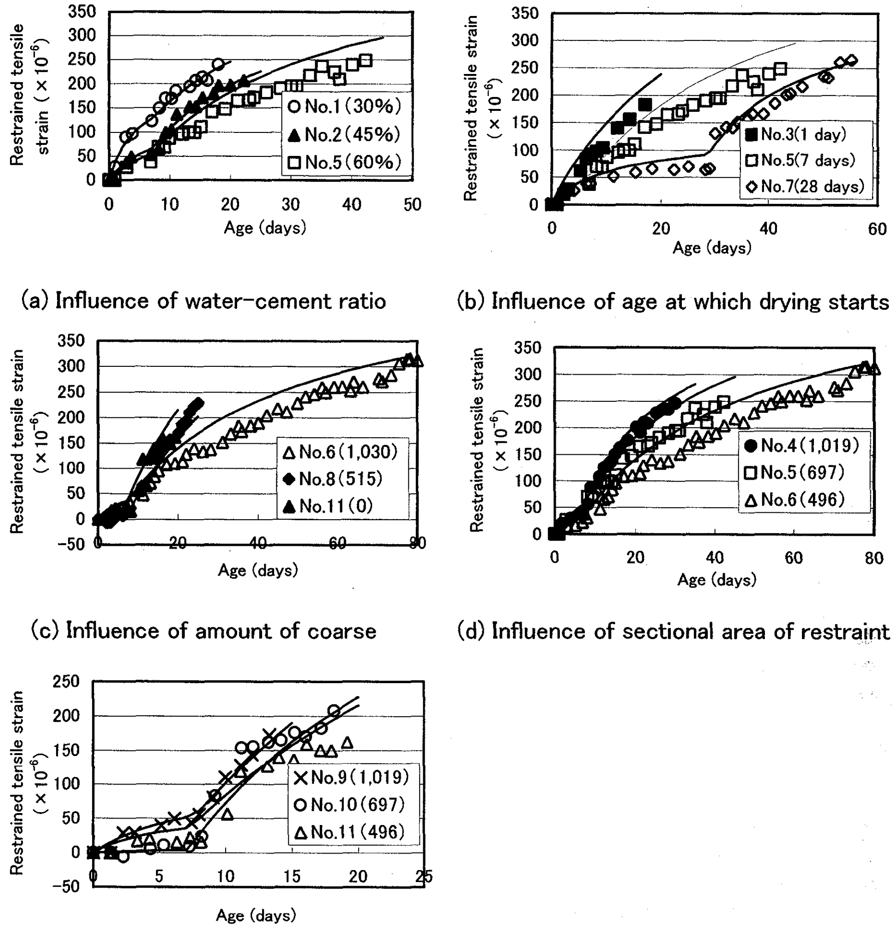

(a) Influence of water-cement ratio

(b) Influence of age at which drying starts

(c) Influence of amount of coarse

(d) Influence of sectional area of restraint

(e) Influence of sectional area of restraint frame

Fig. 22 Comparison of calculated values with measured values of restrained tensile strain

$$\phi(t,t_0)=\phi_0\cdot\beta_c(t-t_0) \tag{12}$$

Here, $\phi(t,t_0)$ is creep coefficient and t is age of concrete [days] at the moment under consideration. And t_0 is age of concrete [days] at loading, ϕ_0 is notional creep coefficient in Equation (13), and β_c is coefficient to describe the development of creep with time after loading Equation (17).

$$\phi_0=\phi_{RH}\cdot\beta(f_{cm})\cdot\beta(t_0) \tag{13}$$

$$\phi_{RH}=1+\frac{1-RH/RH_0}{0.46(h/h_0)^3} \tag{14}$$

$$\beta(f_{cm})=\frac{5.3}{(f_{cm}/f_{cmo})^{0.5}} \tag{15}$$

$$\beta(t_0)=\frac{1}{0.1+(t_0/t_1)^{0.2}} \tag{16}$$

$$\beta_c(t-t_0)=\left[\frac{(t-t_0)/t_1}{\beta_H+(t-t_0)/t_1}\right]^{0.3} \tag{17}$$

It is clear from Fig.22 that the calculated values correspond well with the measured values, though there are some experimental cases for which the correlation is less good, such as experiments No.5 and No.6. In cases where the match is poor, the deviation begins before the age of 20 days, and there is a tendency for any initial difference to propagate over the long term. Therefore, it can be concluded that shrinkage stress and restrained tensile strain can be estimated with practical precision, even if the creep coefficient is based on the assumption that creep strain is proportional to elastic strain, and though autogenous shrinkage and drying shrinkage both operate in concrete, and concrete is exposed under conditions where the stress is greater than the ratio of shrinkage stress to tensile strength of 0.4 (the model code mentioned above is intended for use when the stress-to-strength ratio is under 0.4.).

Time histories of restrained tensile strain obtained by analysis and the curve of tensile strain capacity are plotted together in Fig.23. Here, additional curves are plotted to show variations of plus and minus 10% from the calculated time histories, because the experimental results for restrained tensile strain include an error of about 10%. If tensile strain capacity is adopted as critical cracking limit, then cracking is assumed to occur when the restrained tensile strain reaches the curve of tensile strain capacity.

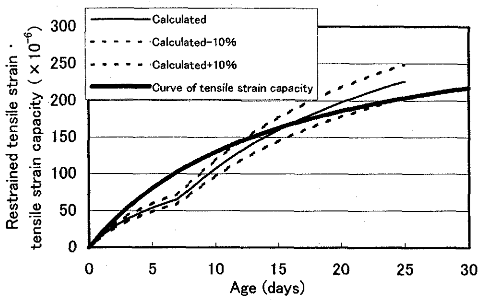

(a) No.2 (W/C=45%)

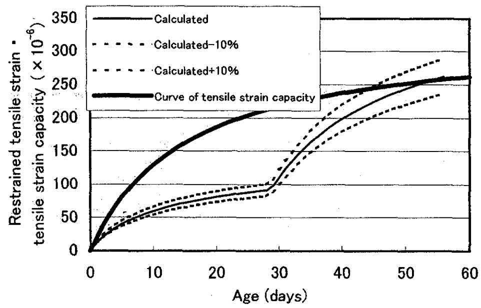

(b) No.7 (Drying starts at 7 days)

Fig.23 Estimation of age at cracking

It is clear from these two figures that the age at cracking is estimated at somewhere between 12 and 25 days in the case of experiment No.2 (as shown in Fig.23 (a)) and that is between 45 and 70 days in the case of experiment No.7 (Fig.23 (b)). In the experiments, the equivalent measured results were within 17.6 to 23.2 days and 45.5 to 57.0 days, respectively, and it can be concluded that the measured age was located within the range of cracking age obtained by the analysis.

The wider range of the estimation increasing time until cracking can be understood because the gradient of the tensile strain capacity curve becomes smaller with time, while the curve of restrained tensile strain also becomes flatter. Therefore, it is not unreasonable that the age at cracking is predicted with lower precision in the case of later cracking.

If the tensile strain capacity curve can be improved in accuracy or if it were to be obtained separately for each mix proportion, and if the restrained tensile strain were calculated in accordance with free-shrinkage strain and Young's modulus as measured in a simple test, then occurrence of cracking can be predicted by using tensile strain capacity as a critical cracking limit as described above.

6. CONCLUSION

Specimens were prepared with various parameters for uni-axial restraint experiments, and tests of cracking under restraint due to autogenous shrinkage strain and drying shrinkage strain were carried out. An analytical approach was also implemented. The following conclusions were reached:

1) Penetrating cracks occur at an earlier age with a lower water-cement ratio, a higher sectional area of the restraint frame, a higher coarse aggregate content, and a shorter wet curing period of 2 days.
2) Restrained shrinkage strain in a uni-axially restrained specimen is not uniform over the cross section of the concrete, and variations in the restrained shrinkage strain over the cross section result in a variance in cracking age even under the same experimental conditions.
3) The area in which strain is released when a penetrating crack occurs ranges over all measurement points on a uni-axially restrained specimen, and this area released from strain has an influence on cracking.
4) The tensile strain capacity, as calculated from the area with an influence on cracking, and the ratio of shrinkage stress to tensile strength (taking into account the development of strength) both increase with increasing time till cracking, and the occurrence of cracking can be predicted by using this trend.
5) Minute cracks immediately lead to penetrating cracks when the ratio of shrinkage stress to tensile strength is 50% to 60% in concrete at an early age, because the pore structure and/or the bond strength between mortar and coarse aggregate have not developed sufficiently.
6) Shrinkage stress and restrained tensile strain can be estimated with practical precision even if the creep coefficient is determined on the assumption that creep strain is proportional to elastic strain, through autogenous shrinkage and drying shrinkage take place in concrete and concrete is exposed to conditions where the stress is higher than the ratio of shrinkage stress to tensile strength of 0.4.

Acknowledgement

We would like to thank Mr. T. Iyoda, in his fourth year at Sibaura Institute of Technology at the time, for his unusual level of cooperation and contribution in performing the experiments.

References

[1] Morinaga, S., "State of Art on Technique of Control of Cracking, Countermeasures and Effect ", Concrete Journal, Vol.34, No.8, pp.13-20, 1996.8 (in Japanese)
[2] JSCE, "Standard Specification for Design and Construction of Concrete Structures [Construction]", 1996.3 (in Japanese)
[3] Makizumi, T., and Tokumitsu, Y., "Study on Cracking Condition of Concrete due to Drying Shrinkage", Proc. of JCI, Vol.5, pp.185-188, 1983 (in Japanese)
[4] Hisaka, M., Mano, K., Yasuda, M., and Kanda, A., "Study on Restrained Cracking Test Method due to Drying Shrinkage", Proc. of Cement and Concrete (Japan Cement Association), Vol.42, pp.419-422, 1988(in Japanese)
[5] Suzuki, N., Ohno, Y., andMiura, Y., "Restrained Cracking Test on Concrete and Properties of Restrained Cracking in Wall", Proc. of JCI, Vol.10, pp.261-266, 1988 (in Japanese)
[6] Ohno, T., and Uomoto, T., "Critical Limit of Concrete Cracking due to Drying Shrinkage", Proc. of JCI, Vol.19, No.1, pp.733-738, 1997 (in Japanese)
[7] Ohno, T., and Uomoto, T., "Influence of Amount of Coarse Aggregate on Concrete Cracking due to Drying Shrinkage", Proc. of Annual Conference of JSCE, No.52, V- pp.1056-1057, 1997 (in Japanese)
[8] Shiire. T., Aoyagi. M., and Kawase, K., "Testing Method on Cracking of Concrete due to Restrained Drying Shrinkage (draft)", Concrete Journal, Vol.23, No.3, pp.50-51, 1985.3 (in Japanese)
[9] Society for the Research of Cracking, "Testing Method on Cracking of Concrete due to Restrained Drying Shrinkage (draft)", Journal of Cement Concrete, No.536, pp.66-68, 1991.10 (in Japanese)
[10] JCI, "Committee Report on Autogenous Shrinkage, Testing Method for Autogenous Shrinkage and Autogenous Expansion of Cement paste, Mortar and Concrete", 1996.11 (in Japanese)
[11] Makizumi, T., and Ohta, T., "Basic Study on Concrete Cracking due to External Restrained Drying Shrinkage", Proc. of JSCE, No.378, 1987.2 (in Japanese)
[12] Society for the Research of Cracking, "Standardization of Testing Method on Restrained Cracking due to Drying Shrinkage and Applicability –Part 3-", Journal of Cement Concrete, No.534, pp.57-65, 1991.8 (in Japanese)
[13] Hisaka, M., Mano, K., Masuda, Y., Yasuda, M., and Kanda, A., "Influence of Water-Cement Ratio on Cracking of Concrete", Proc. of Cement and Concrete (Japan Cement Association), Vol.44, pp.782-787, 1990 (in

Japanese)
[14] Yasuda, M., Abe, M., Sasahara, A., and Momoya, T., "Shrinkage Properties and Cracking for Various Highly Flowable Concrete", Proc. of JCI, Vol.18, pp.147-152, 1996 (in Japanese)
[15] Society for the Research of Cracking, "Standardization of Testing Method on Restrained Cracking due to Drying Shrinkage and Applicability –Part 2-", Journal of Cement Concrete, No.533, pp.56-66, 1991.7 (in Japanese)
[16] Suzuki, N., Ohno, Y., Nakagawa, T., and Ohta, H., "Test of Restrained Cracking due to Shrinkage, Proc. of JCI, Vol.3, pp.25-28, 1981 (in Japanese)
[17] Hayashida, T., Ohno, Y., and Nakagawa, T., "Influence of Reinforcement and Length of Specimen on Autogenous Shrinkage Stress", Proc. of JCI, Vol.21, No.2, pp.733-738, 1999 (in Japanese)
[18] Tokumitsu, Y., and Makizumi, Y., "Analytical Method of Shrinkage Stress to Predict Cracking due to Drying Shrinkage", Proc. of JCI, Vol.6, pp.429-432, 1984 (in Japanese)
[19] Mano, K., Hisaka, M., and Kawase, K., "Influence of Kind of Aggregate on Concrete Cracking due to Drying Shrinkage", Proc. of Cement and Concrete, Vol.42, pp.423-426, 1988 (in Japanese)
[20] Society for the Research of Cracking, "Standardization of Testing Method on Restrained Cracking due to Drying Shrinkage and Applicability –Part 1-", Journal of Cement Concrete, No.532, pp.49-56, 1991.6 (in Japanese)
[21] JCI, "Points in Concrete Technology '94", 1994 (in Japanese)
[22] CEB－FIP, "MODEL CODE 1990", 1990